Asian Journal of Information Technology 15 (15): 2702-2708, 2016
ISSN: 1682-3915

Kernel SVM Classifier for Detection of Glaucoma Using LBP Based Fractal Features

[1]K. Nirmala, [2]N. Venkateswaran and [2]C. Vinoth Kumar
[1]Department of Biomedical Engineering,
[2]Department of Electronics and Communication Engineering,
SSN College of Engineering, Chennai, Tamil Nadu, India

Abstract: Glaucoma refers to the optic nerve damages, causing functional abnormalities in the visual field leading to irreversible loss of vision. The diagnosis of glaucoma at an early stage becomes vital to prevent the damage to optic nerve. In a fundus image, glaucoma is well characterised by recognizable patterns of optic disc and retinal nerve fibre structure. In this study, we present a methodology for diagnosis of glaucoma by using the Local Binary Patterns (LBP) and fractal features from fundus image. The input fundus image is pre-processed using Contrast Limited Adaptive Histogram Equalisation method (CLAHE). The LBP of the enhanced image is obtained and fractal features are extracted from the LBP. Significant fractal feature are selected based on the t-test statistics. Finally, Kernel based Support Vector Machine classifier (K-SVM) is employed on the selected features for classifying the healthy and glaucomatous image. The presented methodology is implemented with the images obtained from FAU and RIMONE database. Simulation results, demonstrate that the fractal features obtained from LBP with K-SVM Classifier identifies glaucomatous eye with higher accuracy when compared with clinical results.

Key words: Glaucoma, histogram equalisation, local binary pattern, fractal features, support vector machine

INTRODUCTION

Glaucoma is an eye disease that is caused by Increased intraocular Pressure (IOP) due to blocking of the drainage channels in the eye. It is characterised by gradual loss of visual function and finally leading to complete blindness. No early symptoms will be known until a significant vision loss has occurred. The main features associated with glaucoma are increased IOP, changes in the structure of optic nerve head and retinal nerve fibre layer thickness. Screening for glaucoma includes certain techniques like tonometry, gonioscopy and colour fundus photography. In tonometry and gonioscopy methods, the presence of glaucoma can be identified only at its advanced stage of the disease whereas regular screening of the eye with colour fundus imaging detects the presence and progression of the disease at its early stage. Commonly used parameters for the analysing the presence and progression of glaucoma are using colour fundus imaging are increased cup to disk ratio, development of disk pallor, thinning of neuro retinal rim and displacement of retinal blood vessel. Glaucoma progression can still be classified from textural features by applying digital image analysis such as orthogonal decomposition methods. The texture features and higher order spectra can also be used for glaucomatous image classification. Enhancement technique was proposed (Yoon *et al*., 2009) which divides the input image histogram into sub histogramsand performed Histogram Equalisation (HE) in each sub histogram. An image enhancement technique for detection of Optic Disc (OD) using canny edge detection filter was presented (Hatanaka *et al*., 2011). Template based method for optic disc segmentation was proposed (Aquino *et al*., 2010). In this approach, the approximate OD boundary is obtained using morphological operation, edge detection and circular transform. A method to segment OD by active contour model and optic cup segmentation based on the bending of retinal blood vessels was presented (Joshi *et al*., 2011). In this method, Glaucoma assessment is obtained by calculating the ratio between optic cup and disc area. A system to classify glaucoma using wavelet based energy features and neural network was suggested (George, 2013). A detailed literature study on pre-processing, feature extraction, feature selection and various machine learning techniques for detection of glaucoma was presented (Khalil *et al*., 2014). The researchers have concluded that the Naive Bayes and Line regression based classification have good accuracy. System was proposed based on hybrid feature extraction

Corresponding Author: K. Nirmala, Department of Biomedical Engineering, SSN College of Engineering, Chennai, Tamil Nadu, India

from fundus image using higher order spectra, trace transform and Support Vector Machine (SVM) classifier. Texture analysis based on Local Binary Patterns (LBP) and Gaussian Markov random field approach that provides textural features with quantitative representation of retinal nerve fibre layer texture was presented (Novotny *et al*., 2010). The derivatives of LBP such as multivariate LBP, centre symmetric LBP, LBP variance, dominant LBP, advanced LBP, Local Texture Pattern (LTP) and Local Derivative Pattern (LDP) was proposed for face recognition (Suruliandi *et al*., 2012). The use of a combination of texture and colour features for the classification of Dermoscopy images was proposed (Riaz *et al*., 2014). The texture features consist of a variation of LBP in which the strength of the LBPs is used to extract scale adaptive patterns at each pixel followed by the construction of a histogram. An automatic method based on local texture features extracted from fundus photographs for detection of glaucoma was presented. It implements the complete modelling of LBP to capture representative texture features like LBPM and LBPC. With Nearest neighbour technique is used for classification. The Texture spectrum model based LBP for OD segmentation and various unsupervised clustering approaches like Expectation Maximization (EM), k-means and Fuzzy C Means for OC segmentation to calculate CDR for glaucoma detection (Thulasi and Sikamani, 2015) was presented.

A method for detecting the glaucomatous eye with fractal dimension as features for retinal nerve fibre losses detection using SVM classifier was presented (Kolar and Jan, 2008). A method was introduced (Lamani *et al*., 2013) to extract the fractal dimension features using two algorithms namely semi-variance and box counting for early detection of Glaucoma. The use of Fractal Analysis (FA) as the basis for multiclass prediction of the progression of Glaucoma using a box-counting method and a multi fractional Brownian motion method that incorporates texture and multiresolution analyses was investigated (Kim *et al*., 2013). A method to measure the distribution of the image intensity using fractal dimension. Box dimension, correlation dimension and information dimension are applied in the construction of fractal features (Zhou and Liang, 2014). The object is recognised based on the similarity of box, correlation and information dimensions from the fractal features.

MATERIALS AND METHODS

In this study, the colour fundus image is pre-processed using Contrast-Limited Adaptive Histogram Equalization (CLAHE) and the Region of Interest (ROI), the OD is localised. LBP is applied to the enhanced ROI. Fractal features like fractal Dimension (D), D-dimensional area (A), fractal model Fitting Error (FE), Multi-scale Fractal Feature Related with D (MFFD), multi-scale Fractal Feature Related with K (MFFK), Fractal Abundance (FA) and Lacunarity (LC) are obtained from the LBP images. The features are given to the kernel based SVM classifier for determination of healthy and glaucomatous image. The methodology is shown in Fig. 1.

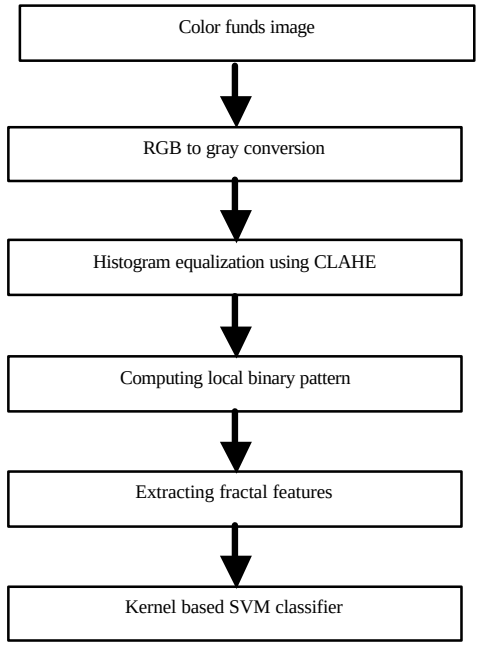

Fig. 1: Block diagram of the proposed system; a, b) input image

Image enhancement: Pre-processing is carried out to aid the extraction of morphological features from the fundus image. Contrast enhancement improves the discrimination of the retinal features. CLAHE is implemented for adjusting the image intensities to have uniform distribution on the histogram. CLAHE is applied to gray scale fundus image to obtain enhanced image. The optic disk dimension, colour and shape aids detection of glaucoma. The OD region is the brightest in fundus image and has maximum number of high intensity pixels. The OD region is localised by dividing the image into subblocks and each subblock is analysed for the presence of maximum number of high intensity pixels. The input ROI image is shown in Fig. 2a, b and enhanced ROI is shown.

Local Binary Pattern (LBP): LBP operator transforms an image into an array or image of integer labels describing small-scale appearance of the image. LBP is a local, gray scale invariant texture descriptor widely used in analyzing

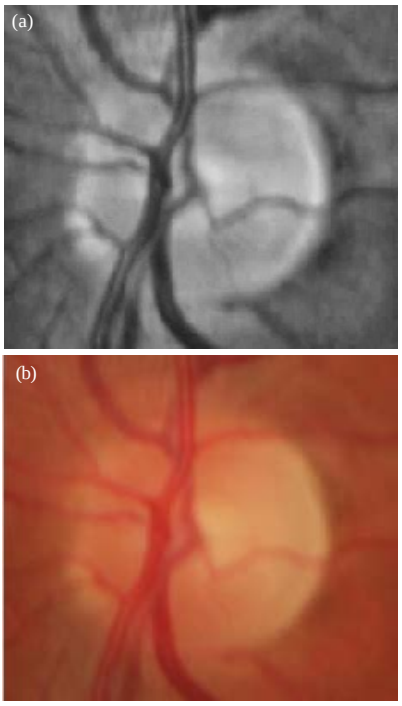

Fig. 2: Enhanced ROI

the differential structure in vision related applications. LBP operator improves classification accuracy. The basic form of LBP works with a set of nine pixels (i.e.,) 3×3 pixel block of the image. The pixels in this block are thresholded by its center pixel value. The center pixel in the matrix is compared with the surrounding neighboring pixels and if the center pixel value is greater than the neighboring pixel then the value of the neighboring pixel is marked as logical 1 otherwise it is marked as logical 0. As result of comparison eight 1 bit values are obtained and then multiplied by powers of two and finally summed to obtain a label for center pixel.

Figure 3 shows the calculation of LBP for a subblock of size 3×3. The mathematical operation of the LBP is given in Eq. 1:

$$LBP(i,r) = \sum_{i=0}^{i-1} s(n_i - c_p)2^i \quad (1)$$

Where:

n_i = The intensity of the neighboring pixels
c_p = The intensity of the center pixel
i = The number of the neighboring pixels
r = The radius of the block size

The function s (ni-cp) is given in Eq. 2:

$$s(n_i - c_p) = \begin{cases} 1 & n_i > c_p \\ 0 & n_i < c_p \end{cases} \quad (2)$$

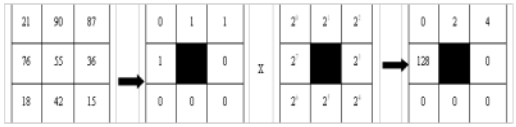

Fig. 3: LBP calculation for 3×3 subblock

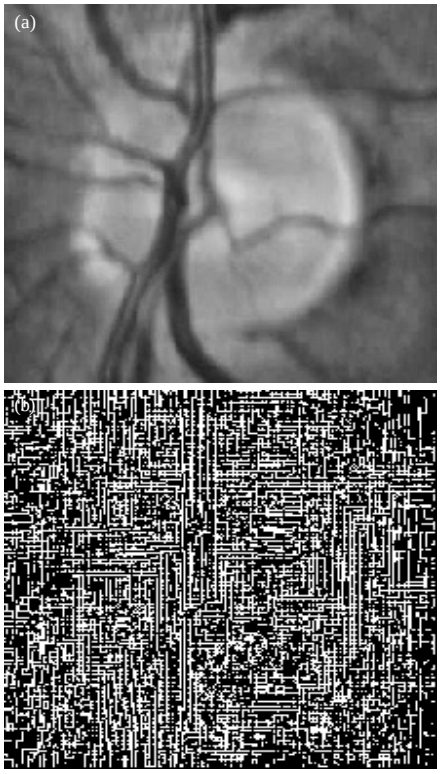

Fig. 4: a) Enhanced ROI and b) LBP image of enhanced ROI

The LBP operator is implemented in the enhanced ROI and the output is shown in Fig. 4.

Fractal feature extraction: Fractals are repeating patterns that are self-similar at all scales of magnification and produce irregular shapes and surfaces that cannot be represented by standard geometry. The fractal features have distinct characteristic in differentiating the normal and glaucoma subjects. In this study, the following fractal features are extracted from the retinal images.

Fractal dimension and fractal abundance: Fractal dimension is the measure of distribution of gray values in an image. The complexity of an object can be measured through fractal dimension. The fractal dimension is calculated from the intensity of the image by using Hausdorff dimension method. It gives a quantitative

measure of self-similarity and scaling. The Hausdorff method to calculate the fractal dimension is as follows:

- Resize the image by padding it with the background pixels to have dimension in power of 2
- Set the box size 'e' to the size of the image
- Compute N(e) which corresponds to the number of boxes of size 'e' which contains at least one object pixel
- If e>1, then e = e/2 and repeat step 3
- Compute the points log (N(e) x log(1/e) and use the least squares method to fit a line to the points
- The returned Hausdorff fractal dimension is the slope of the line
- The intercept of the line gives the fractal abundance

The fractal dimension is computed from the slope of the line drawn between number of the logarithmic value of the occupied boxes (log N e) versus the logarithmic values of the size of the box (log 1/e). The line drawn for an image is shown in Fig. 5. The slope of the line gives the fractal dimension for that single image.

D Dimensional area and fractal model fitting error: The D dimensional area and fractal model fitting error of an image depend on the surface area of the image at different scales. The D dimensional area can be calculated using (Eq. 3):

$$A(\varepsilon) = k\varepsilon^{2-D} \tag{3}$$

Where:
D = Fractal dimension
k = Proportionality constant and $\epsilon = 2, 4, 8, \ldots, \epsilon_{max}$
ϵ_{max} = The maximum size of the image

The D dimensional area is the slope of the line that is obtained by linear fitting for log (A(x, y, ϵ) at each scale ϵ. The fractal model fitting error is computed from surface area at each scale as shown in Eq. 4:

$$FE = \sum_{\varepsilon=1}^{\varepsilon_{max}} \left| \log(A(x,y,\varepsilon)) - (2-D)\log(\varepsilon) - \log(K) \right| \tag{4}$$

Multi-scale fractal features: The Multi-scale fractal features are obtained by calculating the fractal dimension and D dimensional area for each scale. The values of these features are different between the normal and abnormal regions of fundus image, so that they can be classified with better accuracy. The fractal dimension at each scale is obtained from Eq. 5:

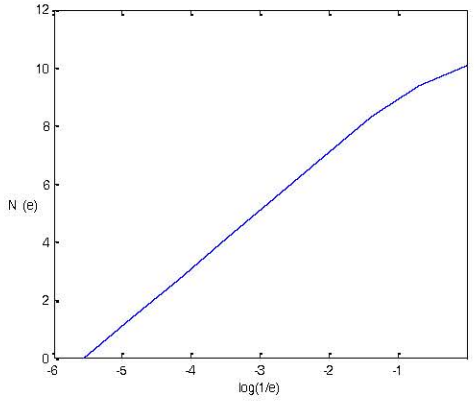

Fig. 5: Illustration of fractal dimension for an image

$$D(x,y,\varepsilon) = 2 - \left\{ \frac{\log(A(\varepsilon)) - \log(A(\varepsilon-1))}{\log(\varepsilon) - \log(\varepsilon-1)} \right\} \tag{5}$$

The Multi-scale fractal dimension is given by Eq. 6:

$$MFFD = \sum_{\varepsilon=2}^{\varepsilon_{max}} \left(D(x,y,\varepsilon) - \frac{1}{\varepsilon_{max}-1} \sum_{\varepsilon=2}^{\varepsilon_{max}} D(x,y,\varepsilon) \right)^2 \tag{6}$$

Where:
A' = log (A(ϵ-1)
ϵ' = log (ϵ-1)

The D dimension area at each scale can be obtained from Eq. 7:

$$K(\varepsilon) = \exp\left(\frac{\varepsilon' \log(A(\varepsilon)) - A' \log(\varepsilon)}{\log(\varepsilon-1) - \log(\varepsilon)} \right) \tag{7}$$

The multi-scale D dimension area is given by Eq. 8:

$$MFFD = \sum_{\varepsilon=2}^{\varepsilon_{max}} \left(K(x,y,\varepsilon) - \frac{1}{\varepsilon_{max}-1} \sum_{\varepsilon=2}^{\varepsilon_{max}} K(x,y,\varepsilon) \right)^2 \tag{8}$$

Lacunarity: The lacunarity is a function of box size that represents the distance between patterns. The fractal lacunarity is given in Eq. 9:

$$\Lambda(L) = \frac{M^2(L) - (M(L))^2}{(M(L))^2} \tag{9}$$

$$M(L) = \sum_{m=1}^{N} mp(m,L) \tag{10}$$

Table 1: Fractal features for normal fundus

Images	FD	FE	D-Dim area	MFFD	MFFK	FA	LC
Image 1_N	1.8764	19.6551	8.0935	3.4119	2.49E+21	10.5942	1.3394
Image 2_N	1.8894	18.2386	8.0405	3.4591	3.13E+20	10.6477	1.3125
Image 3_N	1.8894	18.2367	8.0419	3.4592	3.12E+20	10.6479	1.3082
Image 4_N	1.8847	18.7365	8.6744	3.4420	1.02E+21	10.6285	1.3125
Image 5_N	1.8825	18.9728	8.5142	3.4341	1.29E+21	10.6195	1.3337
Image 6_N	1.8801	19.2447	8.3395	3.4251	1.68E+21	10.6093	1.3340
Image 7_N	1.8805	19.1946	8.3710	3.4268	1.60E+21	10.6113	1.3495
Image 8_N	1.8696	20.4571	7.6659	3.3869	2.25E+21	10.5657	1.3768
Image 9_N	1.8883	18.3541	8.9518	3.4551	2.91E+20	10.6432	1.3115
Image 10_N	1.8791	19.3527	8.2728	3.4216	1.86E+21	10.6050	1.3470

Table 2: Fractal features for glaucomatous images

Images	FD	FE	D-Dim area	MFFD	MFFK	FA	LC
Image 1_G	1.8918	16.9842	9.2443	3.2680	4.71E+20	11.6578	1.1992
Image 2_G	1.8899	17.1867	9.0810	3.2609	5.81E+20	12.6498	1.1024
Image 3_G	1.8930	16.8657	9.3434	3.2722	4.16E+20	11.6627	1.0104
Image 4_G	1.8890	16.2804	9.0081	3.2576	6.40E+20	11.6466	1.1231
Image 5_G	1.8874	16.4434	9.8849	3.1520	7.57E+20	12.6401	1.0041
Image 6_G	1.8900	17.1718	9.0928	3.2614	5.73E+20	11.6505	1.0078
Image 7_G	1.8927	17.8897	9.3231	3.1714	4.27E+20	12.6617	1.1976
Image 8_G	1.8902	17.1584	9.1033	3.1619	5.65E+20	12.6511	1.0122
Image 9_G	1.8875	16.4399	9.8875	3.2521	7.54E+20	12.6400	1.0130
Image 10_G	1.8913	17.0405	9.1981	3.2660	5.00E+20	11.6557	1.1041

$$M^2(L) = \sum_{m=1}^{N} m^2 p(m, L) \quad (11)$$

Where:

L = Box size

N = The number of possible intensity points within the box size L

m = The intensity point within the box

p (m, L) = The probability of that intensity point

Kernel based Support Vector Machine (K-SVM): The SVM is a supervised learning algorithm that analyzes data and recognizes the patterns for classification. It is based on the statistical learning theory for classification. The mathematical model for SVM is given in Eq. 12:

$$f(x) = w^T x + b \quad (12)$$

Where:

w = The unit vector

b = The constant

The linear SVM can be extended to a nonlinear classifier by the use of a nonlinear kernel (K). The K-SVM approach is a nonlinear classifier in which the training vector x_i is mapped to higher dimensional feature space through nonlinear kernel function. The output of SVM is a linear combination of the training examples projected onto a high-dimensional feature space through the kernel functions. Performance of the classification can be improved by providing more information obtained by mapping the high dimension space with nonlinear kernel function. One of popular kernel function is Radial Basis Function (RBF). The nonlinear SVM classifier is given in Eq. 13:

$$f(x) = w^T K(x) + b \quad (13)$$

The RBF which is used as nonlinear kernel function is given in Eq. 14:

$$K(x, y) = \exp\left(\frac{\text{norm}(x - y)^2}{\sigma^2}\right) \quad (14)$$

Performance and simulation results: The simulation results were obtained by using normal and glaucoma images from FAU and RIMONE database. RIMONE database is exclusively focused on the optic nerve head segmentation, composed of high resolution 169 full fundus healthy and glaucoma progressing images. FAU database composed of healthy and glaucoma images obtained using canon CR-1 fundus camera with a field of view 45°. The retinal fundus images are enhanced by CLAHE method. The enhanced images are divided into subblocks of size 32×32 (to cover the entire OD region) and the presence of maximum number of high intensity pixels is localized as ROI. LBP is computed on ROI and the Fractal features are computed. The extracted fractal features values for the normal fundus images (Image 1_N to 10_N) and glaucoma images (Image 1_G to 10_G) are tabulated in Table 1 and 2.

From the extracted features, the best feature is selected for further classification process. The extracted fractal features are ranked by performing‘t test’ and the ‘t’ value for all the extracted features are tabulated in Table 3. Out of seven fractal features two significant

Table 3: 't' test values for fractal features

Fractal features	Normal	Glaucoma	't' values
LC	1.331700	1.0639000	10.883800
FA	10.619700	12.2065000	10.067600
MFFD	3.434400	3.2284000	9.129900
FE	18.976400	16.9418000	7.047100
D Dim Area	8.319100	9.3247000	5.944400
FD	1.876400	1.8918000	3.381100
MFFK	1.18E+21	5.7922E+20	2.404271

Table 4: Performance measures of K-SVM classifier with fractal features

Fractal features	TPR (%)	TNR (%)	FPR (%)	FNR (%)	ACC (%)	PPV (%)
FD	92	76	24	8	79.0	73.0
FE	92	75	25	8	78.5	72.4
K	91	79	21	9	80.0	74.5
MFFD	92	76	24	8	79.0	73.0
MFFK	99	73	27	11	73.0	65.6
FA	92	84	16	8	88.5	82.9
LC	87	89	11	13	88.0	86.6

features namely the lacunarity and fractal abundance are fed to the classifier for identifying the given input images as normal or glaucomatous. The selected fractal features are fed to K-SVM classifier. The classifier includes separate phases of training and testing which is implemented by cross validation method. An n-way cross validation breaks the entire data set into n more-or-less equal parts. From each part, one data is randomly selected as test data and other data are used as training data. This gives n results and the over all result is the average of those n results (here n = 10). The retinal data set has 200 samples in all, so a 10-way cross validation would provide a convenient partitioning into 10 groups of 20 images each. The performance of the classifier is validated using True Positive Rate (TPR), True Negative Rate (TNR), False Positive Rate (FPR), False Negative Rate (FNR), Accuracy (ACC) and Positive Predictive Value (PPV) measures. The ACC and PPV value are obtained using Eq. 15 and 16:

$$ACC = \frac{TPR + TNR}{TPR + FPR + FNR + TNR} \quad (15)$$

$$PPV = \frac{TPR}{TPR + FPR} \quad (16)$$

Where:

TPR = The number of normal samples correctly identified (sensitivity)

FNR = The number of normal samples incorrectly identified as glaucoma (specificity)

FPR = The number of glaucoma samples incorrectly identified as normal

TNR = The number of glaucoma samples correctly identified

The performance measures of K-SVM classifier for the fractal features extracted from LBP image is shown in Table 4. By extracting the fractal features from the LBP

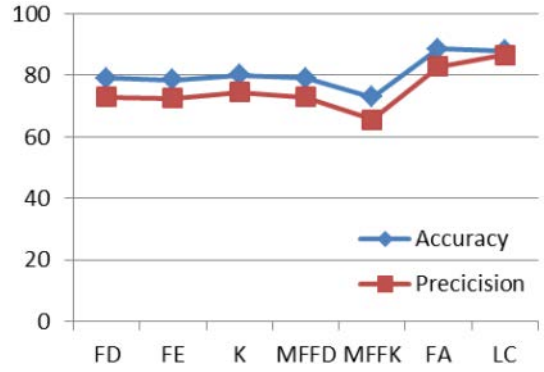

Fig. 6: Performance graph for fractal features

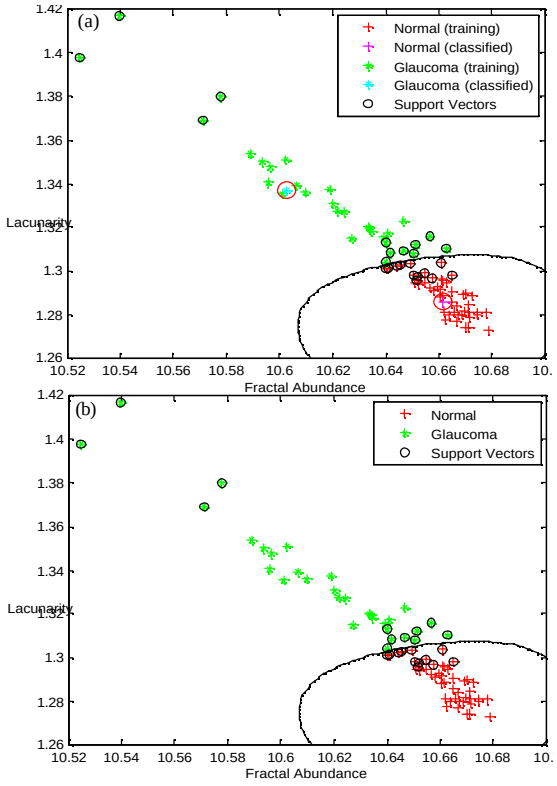

Fig. 7: Hyper plane: a) training and b) testing

image, K-SVM classifier differentiates the normal and glaucoma images with an accuracy of 89% and precision of 86%. Fractal abundance and lacunarity features have highest ACC and PPV compared to the other fractal features as depicted in Fig. 6. The hyper plane obtained by using RBF as kernel is shown in Fig. 7a, b. The training of K-SVM classifier with healthy and glaucomatous images based on significant fractal feature is shown in Fig. 7a. The testing of the classifier with one normal and glaucoma image is depicted in Fig. 7b confirms that K-SVM accurately classifies input test images.

CONCLUSION

In this study, K-SVM classifier for detection of Glaucoma using LBP based fractal features is presented. CLAHE is used to enhance the input retinal images. The LBP image is obtained from the enhanced image and fractal features are computed from the LBP image. Significant fractal features such as lacunarity and fractal abundance are selected from the extracted features and then fed to K-SVM classifier. Ten-fold cross method is implemented to validate the classifier. The fractal features in combination with the LBP technique gives better discrimination between the normal and glaucoma images.Simulation results confirm that the K-SVM classifier with LBP based fractal features gives a classification accuracy of 89%. The fractal features can also be used in the screening program together with other features obtained from different texture analysis methods.

REFERENCES

Aquino, A., M.E. Gegundez-Arias and D. Marin, 2010. Detecting the optic disc boundary in digital fundus images using morphological, edge detection and feature extraction techniques. IEEE Trans. Med. Imag., 29: 1860-1869.

George, C.R., 2013. Glaucomatous image classification using wavelet based energy signatures and neural networks. Int. J. Eng. Res. Technol., 2: 1-5.

Hatanaka, Y., A. Noudo, C. Muramatsu, A. Sawada and T. Hara *et al*., 2011. Automatic measurement of cup to disc ratio based on line profile analysis in retinal images. Proceedings of the 2011 Annual International Conference of the IEEE Engineering in Medicine and Biology Society, August 30-September 3, 2011, IEEE, Boston, Massachusetts, ISBN: 978-1-4244-4121-1, pp: 3387-3390.

Joshi, G.D., J. Sivaswamy and S.R. Krishnadas, 2011. Optic disk and cup segmentation from monocular color retinal images for glaucoma assessment. IEEE. Trans. Med. Imag., 30: 1192-1205.

Khalil, T., S. Khalid and A.M. Syed, 2014. Review of machine learning techniques for glaucoma detection and prediction. Proceedings of the Conference on Science and Information (SAI), August 27-29, 2014, IEEE, London, England, ISBN: 978-0-9893-1933-1, pp: 438-442.

Kim, P.Y., K.M. Iftekharuddin, P.G. Davey, M. Toth and A. Garas *et al*., 2013. Novel fractal feature-based multiclass glaucoma detection and progression prediction. IEEE. J. Biomed. Health Inf., 17: 269-276.

Kolar, R. and J. Jan, 2008. Detection of glaucomatous eye via color fundus images using fractal dimensions. Radio Eng., 17: 109-114.

Lamani, D., D.R. Ramegowda and D.R.T.C. Manjunath, 2013. Fractal dimension as diagnostic parameter to detect glaucoma. Int. J. Innov. Eng. Technol. IJIET., 2: 63-69.

Novotny, A., J. Odstrcilik, R. Kolar and J. Jan, 2010. Texture analysis Of nerve fibre layer in retinal images via local binary patterns and gaussian markov random fields. Anal. Biomed. Sign. Images, 20: 308-315.

Riaz, F., A. Hassan, M.Y. Javed and M.T. Coimbra, 2014. Detecting melanoma in dermoscopy images using scale adaptive local binary patterns. Proceedings of the 2014 IEEE 36th Annual International Conference on Engineering in Medicine and Biology Society, August 26-30, 2014, IEEE, Chicago, Illinois, pp: 6758-6761.

Suruliandi, A., K. Meena and R.R. Rose, 2012. Local binary pattern and its derivatives for face recognition. IET Comput. Vision, 6: 480-488.

Thulasi, N. and K.T. Sikamani, 2015. Early detection of glaucoma based on local binary pattern and unsupervised clustering approaches using fundus images. Middle East J. Sci. Res., 23: 1632-1638.

Yoon, H., Y. Han and H. Hahn, 2009. Image contrast enhancement based sub-histogram equalization technique without over-equalization noise. World Acad. Sci. Eng. Technol., 50: 176-182.

Zhou, Y. and J. Liang, 2014. Fractal features for object recognition. Proceedings of the 2014 12th International Conference on Signal Processing (ICSP), October 19-23, 2014, IEEE, Hangzhou, China, ISBN: 978-1-4799-2188-1, pp: 1225-1229.